BOLETIN DE LA SOCIEDAD ESPAÑOLA DE
Cerámica y Vidrio
www.elsevier.es/bsecv

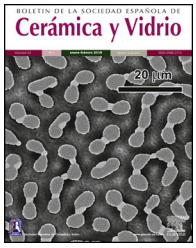

Potentiality of new dark clay-rich materials for porous ceramic applications in Ouled Sidi Ali Ben Youssef Area (Coastal Meseta, Morocco)

Achraf Harrati[a], *Ahmed Manni*[a], *Fahd Oudrhiri Hassani*[b], *Ali Sdiri*[c], *Souad El Kalakhi*[d], *Abdeslam El Bouari*[a], *Iz-Eddine El Amrani El Hassani*[e], *Chaouki Sadik*[a,*]

[a] *Laboratory of Physical Chemistry of Applied Materials (LPCMA), Department of Chemistry, Faculty of Sciences Ben Msik, Hassan II University of Casablanca, Morocco*
[b] *LMPEQ, University of Cadi Ayyad, ENSA of SAFI, Morocco*
[c] *National Engineering School, University of Sfax, P. Box 3052 Sfax, Tunisia*
[d] *EMPM-LPCMI, Faculty of Sciences Aïn Chock, Hassan II University of Casablanca, Morocco*
[e] *Geomaterials and Geo environment Team/Geo-Biodiversity and Natural Patrimony Laboratory, (GEOBIO)/Geophysics, Natural Patrimony and Green Chemistry Research Centre (GEOPAC), Scientific Institute, Mohammed V University of Rabat, Morocco*

ARTICLE INFO

Article history:
Received 27 April 2020
Accepted 5 August 2020
Available online 8 September 2020

Keywords:
Clay
Expanded perlite
Traditional ceramic
Porosity
Insulating

ABSTRACT

Potential use of raw clayey deposits from El Jadida, Morocco, in the manufacture of traditional ceramic products has been evaluated through a careful sampling and an in-depth characterization of the outcropping features around Ouled Sidi Ali Ben Youssef area (El Jadida city). We collected six representative clay-rich materials (C1–C6) for subsequent analyses by several spectroscopic and mineralogical techniques including physico-chemical, mineralogical, and thermal analyses. Our results revealed high amounts of oxides, mainly SiO_2, Al_2O_3, Fe_2O_3, CaO and MgO. Those ferruginous clays were found suitable for dark ceramic bodies. Further mineralogical examination confirmed low to medium contents of clay minerals, but subordinated by quartz, calcite, dolomite and plagioclase as the main nonclay minerals. Ternary diagram plots indicated that the studied clays were suitable for structural clay products and clay roofing tiles. C5 sample exhibited the best physico-chemical and mineralogical properties due to its illitic nature (64%), low quartz content (28%), high plasticity index (32) and lower loss on ignition (10.84%). Therefore, C5 clayey sample was selected as a potential candidate to be mixed with expanded perlite (EP) for the production of insulating ceramics. Specimen were prepared from the new mixture (i.e., C5 and EP) by pressing and firing at 1100 °C. The obtained ceramic bodies were ascertained by addressing their bulk density, water absorption, shrinkage, bending strength, thermal conductivity, structural and mineralogical properties.

* *Corresponding author.*
E-mail address: schawki37@gmail.com (C. Sadik).
https://doi.org/10.1016/j.bsecv.2020.08.003

Potencialidad de nuevos materiales ricos en arcilla oscura para aplicaciones de cerámica porosa en el área de Ouled Sidi Ali Ben Youssef (Meseta costera, Marruecos)

Palabras clave:
Arcilla
Perlita expandida
Cerámica tradicional
Porosidad
Aislante

RESUMEN

El uso potencial de depósitos de arcilla en bruto de El Jadida, Marruecos, en la fabricación de productos cerámicos tradicionales se ha evaluado mediante un muestreo cuidadoso y una caracterización en profundidad de las características de afloramiento alrededor del área de Ouled Sidi Ali Ben Youssef (ciudad de El Jadida). Recolectamos seis materiales representativos ricos en arcilla (C1 a C6) para análisis posteriores mediante varias técnicas espectroscópicas y mineralógicas, incluidos análisis fisicoquímicos, mineralógicos y térmicos. Nuestros resultados revelaron altas cantidades de óxidos, principalmente SiO2, Al2O3, Fe2O3, CaO y MgO. Esas arcillas ferruginosas se encontraron adecuadas para cuerpos de cerámica oscura. Un examen mineralógico adicional confirmó contenidos bajos a medios de minerales arcillosos, pero subordinados por cuarzo, calcita, dolomita y plagioclasa como los principales minerales no arcillosos. Los diagramas de diagrama ternario indicaron que las arcillas estudiadas eran adecuadas para productos de arcilla estructural y tejas de arcilla. La muestra C5 exhibió las mejores propiedades fisicoquímicas y mineralógicas debido a su naturaleza ilítica (64%), bajo contenido de cuarzo (28%), alto índice de plasticidad (32) y menor pérdida por ignición (10.84%). Por lo tanto, la muestra arcillosa C5 se seleccionó como un candidato potencial para ser mezclado con perlita expandida (EP) para la producción de cerámica aislante. Las muestras se prepararon a partir de la nueva mezcla (es decir, C5 y EP) presionando y disparando a 1100 ° C. Los cuerpos cerámicos obtenidos se determinaron abordando su densidad aparente, absorción de agua, contracción, resistencia a la flexión, conductividad térmica, propiedades estructurales y mineralógicas.

Introduction

It is well-known that illite is one of the most widely used clay for pottery, cement manufacture and tiles preparation [1,2] due to its abundance and suitable application at a low cost. Illite is, therefore, the main clay specie of the 2:1 layered silicate group. The general formula for illite group can be written as $(Si_{4-x}\ Al_x)^{IV}(Al_{2-y}\ Mg_y)^{VI}\ O_{10}\ (OH)_2$, $(x+y)K^+$ with a charge of 0.9 per $O_{10}(OH)_2$, compensated by the interlayer K^+ sheet. As a result of the non-hydrated nature of its interlayer cations, illite is a non-swelling clay mineral, in contrast to some montmorillonites [3].

Morocco is no exception, where illitic clay deposits are abundantly available across the country [4–7]. They correspond to continental deposits or shallow ocean floor sediment, set up during the Triassic and Lower Cretaceous and form layers of a few metres to several hundred metres of thickness. Those clay gave red coloured brick with fine to coarse grain and shows intercalations of greenstone (weathered basalt flows) and evaporites (rock salt, gypsum, sylvite) [4]. However, the extracted illitic clays are generally associated with various impurities that can affect its physical and chemical properties, leading to the limited industrial application. Therefore, we propose to add expanded perlite to overcome such shortcomings. Expanded perlite (EP) finds its appropriate application in insulating ceramics, lightweight aggregates that are in turn, used instead of denser aggregates, or blended with dense aggregates to achieve the desired density and properties [8–12]. Both ingredients will be mixed for potential use in ceramic industry, especially tiles.

Ceramic tiles are produced by a fast firing process of mixtures that include clay, silica sand, calcite, pyrophyllite, feldspar and additives. They are usually used for flooring covering walls and ventilated facades due to their high technological properties (e.g., low thermal conductivity, high mechanical strength and excellent chemical and abrasion resistance) [13–15]. In this context, numerous studies have been carried out to characterize and use various clays, from morocco, in ceramic [16–28]. However, outcropping features of Ouled Sidi Ali Ben Youssef area (El Jadida, Central Morocco) were not subjected to detailed academic characterizations for a possible application in ceramic industry. Thus, special attention has been devoted to the physico-chemical and mineralogical characterization of representative clay samples from the studied site. The most promising sample (C5) was selected for the preparation of light and porous ceramics. Improvement of the final product has been addressed by addition of different amounts of expanded perlite (EP; 0, 10 and 20%) used as an aggregate.

Materials and methods

Materials

The present study was carried out in red colour clay series. They were collected from the Ouled Sidi Ali Ben Youssef site

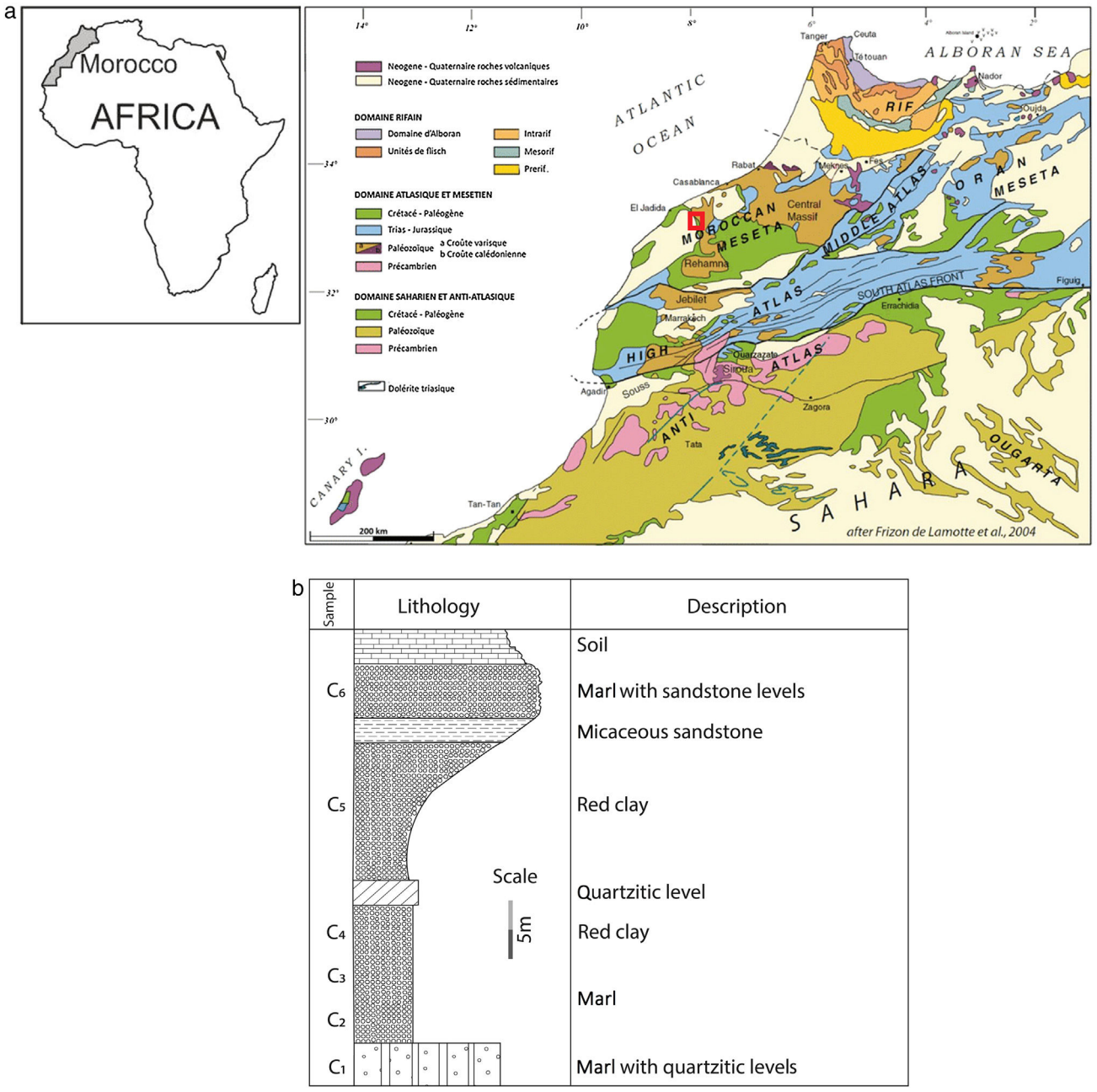

Fig. 1 – (a) Geographic localization of Ouled Sidi Ali Ben Youssef Area on the simplified geological map of Morocco [29] and (b) Synthetic lithostratigraphic log of the studied sector and sampling level (C1–C6).

(Fig. 1a), located about 50 km to the east of El Jadida city where several quarries are being exploited for various industrial applications (e.g., cement, brick, pottery and ceramists). The studied deposit is made by more than 1000 m-thick layer of fine red clays belonging to the Permo-triassic, with quartz/sandstone as the main non clay impurities. Two geological units can be easily recognized from the base upwards: (1) the Autunian base mainly composed of sandstone, conglomerates and red clay; and (2) Permo-Triassic red clay to the top. Our study was carried out on six facies named from the base 'Clay C1' to tops of the section 'Clay C6' (Fig. 1b). Perlite is a hydrated aphanitic volcanic rock of rhyolitic composition. Finely ground and heat treated at around 1000 °C, the perlite expands to give a white, vacuolar and very light material (d = 140–190 kg/m^3). Significant reserves of perlite exist in Morocco, in the Nador region (North of Morocco). But it is not well exploited due to the absence of industrial units for its processing and expansion. Expanded perlite sample was kindly supplied by 'Société d'Etudes et d'Expertise' (CEE) in French.

Characterization techniques

Different characterization techniques including mineralogical analysis by X-ray diffraction (XRD), chemical compositions by X-ray fluorescence (XRF), thermal analysis (TG-DTA) and physical measurement (i.e., granulometry, plasticity) were used for a routine assessment of the main properties of the collected samples. Technological properties were also evaluated for the fired specimens. Chemical analysis of major oxides was determined by X-ray fluorescence spectroscopy (Panalytical Axios spectrometer). The detection limits of each element and the error consideration for analysis have been mentioned. The total amounts of organic matter, both inorganic carbon and interlayer water in phyllosilicates were determined by Loss-On-Ignition at 550 °C for 4 h and at 950 °C for 2 h, respectively. Mineralogical composition of raw materials and high temperature crystalline phases (after firing) was performed by X-ray diffraction using a Xpert Datacollecter software diffractometer with Cu Kα radiations (Kα = 1.5418 Å). Clay fraction (i.e., less than 2 μm fraction) was collected using 10% HCl solution to remove carbonates. It was deflocculated by successive washing with demineralized water and then separated by centrifugation at 9000 rpm for subsequent analyses. Oriented aggregates were mounted on glass slides to minimize the background effects. From XRD patterns, semi-quantitative estimation was performed by the application of the external standard method [30].

FT-IR spectra were obtained with a Bruker Tensor 27 FTIR spectrometer operating in the range 4000–400 cm^{-1}. Laser granulometry has been carried out using the Hydro 2000 instrument, under a darkness of 11.08%, and using water as a light scattered. Thermo-gravimetric curves have been plotted using a Versa-Therm thermo-balance under air atmosphere. Temperature increase from room temperature to 1100 °C was programmed to a regular increment of 10 °C/min. α-Al_2O_3 was used as reference in the temperature range used. Microstructural analysis of the prepared ceramics specimens was conducted by scanning electron micrographs (Hitachi TM3000). For more details on the nature of the mineral phases and microstructure of ceramics, we use the polarized microscope, generally used for petrographic study of natural rocks. For this, we started by making thin slices approximately 30 μm thick in sample fragments. These thin sections have been observed under a microscope Olympus BX 51TF.

$CaCO_3$ contents were measured using a Bernard calcimeter, as described by the French Standard NF P 94-048 (AFNOR, 1996). Atterberg Limits, namely liquid limit (LL) plastic limit (PL), and plasticity index (PI) were evaluated based on Casagrande measurement [31]. Specific Surface Area (SSA) was calculated using the methylene blue index method according to the French Standard NF P 94-068 (AFNOR, 1998). Total organic carbon (TOC) was analyzed by the hydrogen peroxide (H_2O_2) method [20].

Preparation of ceramic bodies

To prepare the desired ceramic products, the collected raw materials (clay and EP) were oven-dried at 105 °C for 24 h before wet grinding to the desired granulometry. Three different granulometric distributions of EP were used including fine (A; less than 200 μm), medium (B; from 400 to 800 μm) and coarse fraction (C; from 1000 to 2500 μm). In total, seven mixtures were prepared and abbreviated as C0, $C10_A$, $C10_B$, $C10_C$, $C20_A$, $C20_B$ and $C20_C$. Where, C refers to clay; 0, 10 and 20 are the percentage addition of EP and subscript letters describe the fraction used (i.e., A, B or C). On a regular basis, the granulated powder mixtures were introduced in a rectangular-shaped mould (10 cm × 5 cm × 1 cm), pressed and then oven-dried at 105 °C for 24 h. Those specimens were introduced to an electrical furnace (Thermolyne 46200) for subsequent firing to 1100 °C at the rate of 5 °C/min; a plateau at 600 °C was set to 1 h dwelling, as described by Sutcu and Akkurt [32].

As for colour measurement, the reddish intensity was determined using the Munsell Soil Colour Chart. The apparent density, water absorption and open porosity were measured according to ASTMC373-88 [33]. Shrinkage measurement was done according to the ASTM C326-03 [34]. Fired products were mechanically characterized with three-point bending. The loading procedure consisted of applying a preliminary load (0.05 kN) at a rate of 0.5 mm/min to eliminate positioning defects of the specimens. Tensile strength was measured by a universal testing machine (UTM) at strain rate 2 mm/min. Thermal conductivity measurements were employed using the Thermal Conductivity Meter (λ-Meter EP500e) [35]. The application of non-destructive methods, based on the measurement of the speed of ultrasonic waves (Vp) was carried out. In this type of non-destructive measurement, wave velocity is determined by measuring the travel time taken by a pulse to get throughout the material. In this study, longitudinal wave velocity of the fired samples is measured by PUNDIT plus PC1006. Dielectric constant measurements were made on disc-shaped samples on a Hewlett Packard HP4284A Precision LCR metre, with a frequency range from 2 to 20 GHz. The abrasion resistance is evaluated by the weight loss of a sample

Table 1 – Mineralogical composition of the studied clays (Q: Quartz, KF: K-feldspar, Pl: Plagioclase, C: Calcite, D: Dolomite, Sd: Siderite, Rh: Rhodochrosite, I: Illite, K: Kaolinite, Ch: Chlorite, Mus: Muscovite, Sm: Smectite, ML: mixed layers).

Samples	Bulk mineralogy (wt.%)									Clay mineralogy (≤2 μm) (wt.%)					
	Clay minerals	Q	K-F	Pl	C	D	Sd	Rh	Fe oxides	I	K	Ch	Mus	Sm	ML
C1	21	48	4	3	9	6	2	2	5	34	12	20	4	–	30
C2	39	31	3	1	7	12	1	1	5	51	13	12	–	8	16
C3	41	32	3	3	10	1	1	1	8	46	15	5	–	8	26
C4	37	41	2	3	4	4	1	–	8	38	18	6	7	5	26
C5	44	28	6	4	4	3	1	1	8	64	19	–	5	12	–
C6	38	26	–	15	13	5	–	–	3	31	18	4	–	10	37

Table 2 – Chemical analyses of the clay raw materials, their <2 μm fraction and expended perlite (in wt.%).

	SiO_2	Al_2O_3	Fe_2O_3	MgO	CaO	K_2O	Na_2O	MnO	TiO_2	P_2O_5	LOI
C1	64.57 ± 0.040	8.77 ± 0.004	4.84 ± 0.005	4.93 ± 0.003	4.12 ± 0.002	2.17 ± 0.004	0.19 ± 0.001	1.14 ± 0.003	0.22 ± 0.002	0.33 ± 0.003	8.23
C1 < 2 μm	52.1	15.6	7.87	4.44	3.55	2.55	0.32	1.13	0.10	–	11.64
C2	51.68 ± 0.030	10.24 ± 0.010	4.29 ± 0.003	8.87 ± 0.006	5.75 ± 0.004	3.10 ± 0.004	0.23 ± 0.001	0.03 ± 0.002	0.16 ± 0.000	0.17 ± 0.000	15.01
C2 < 2 μm	45.03	13.91	6.55	8.03	4.15	3.41	1.33	–	0.14	–	17.4
C3	46.19 ± 0.030	16.13 ± 0.020	7.31 ± 0.009	3.21 ± 0.004	8.97 ± 0.050	3.37 ± 0.003	0.51 ± 0.001	0.08 ± 0.000	0.14 ± 0.000	0.12 ± 0.000	13.36
C3 < 2 μm	42.24	19.31	7.55	2.74	7.33	3.94	1.50	–	–	–	15.30
C4	57.89 ± 0.050	15.39 ± 0.020	7.34 ± 0.010	3.67 ± 0.003	1.44 ± 0.001	2.65 ± 0.002	0.37 ± 0.001	–	0.15 ± 0.000	0.21 ± 0.000	10.87
C4 < 2 μm	51.15	19.81	8.37	3.15	0.9	2.88	0.61	–	0.09	–	12.61
C5	46.45 ± 0.040	22.45 ± 0.030	7.09 ± 0.020	4.87 ± 0.004	2.69 ± 0.001	3.91 ± 0.004	1.13 ± 0.009	0.14 ± 0.000	0.19 ± 0.000	0.17 ± 0.000	10.84
C5 < 2 μm	40.75	28.37	5.61	3.91	2.01	4.55	2.30	0.2	–	–	11.54
C6	44.02 ± 0.050	15.97 ± 0.030	4.61 ± 0.002	6.61 ± 0.002	9.17 ± 0.030	2.83 ± 0.003	1.43 ± 0.001	–	0.23 ± 0.000	0.39 ± 0.001	14.41
C6 < 2 μm	40.21	19.38	6.00	5.01	7.52	1.94	2.61	–	0.1	–	16.74
a	30	5	2	2	0	0	0	0	0	0	
b	90	30	10	10	14	5	2	1	1	0.5	
EP	72.04	14.13	0.65	0.25	0.66	5.14	3.37	0.07	0.09	–	3.21

a maximum value, b minimum value for bulk compositions

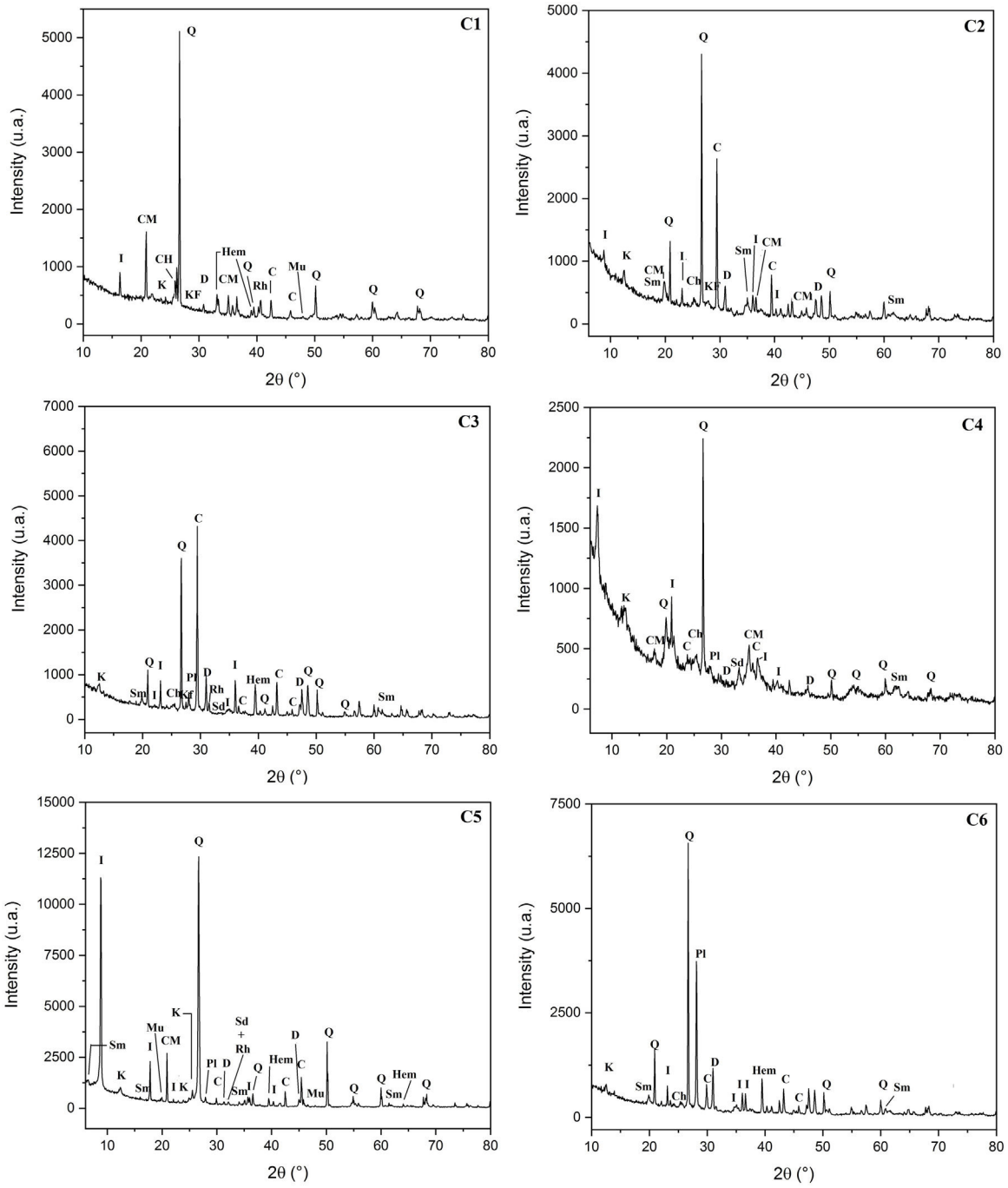

Fig. 2 – XRD patterns of the studied bulk clays. (I: Illite, K: Kaolinite, CH: Chlorite, Sm: Smectite, KF: K-feldspar, D: Dolomite, C: Calcite, Hem: Hematite, Mu: Muscovite, Rh: Rhodochrosite, Sd: Siderite, Q: Quartz, Pl: Plagioclase, CM: Clay minerals).

subjected to abrasion simulated by the brush test (one round trip per second for 1 min). Experiments were run in triplicate to get the average value. All measurements were undertaken at room temperature.

Results and discussion

Characterization of clay materials

The mineralogical composition of bulk samples (size particles > 2 μm) fraction shows that the Moroccan clays includes an average content of clay minerals (21–44%) (Table 1 and Fig. 2). XRD patterns revealed high quartz contents ranging between 26 and 48%. Calcite and dolomite are ubiquitously present (9–21%) with subordinate amounts of siderite and rhodocrosite. In the C6 clay sample, quartz was slightly low (26%), corresponding to the highest carbonates content (18%). The highest clay content was found in the C5 clay sample (44%). Table 1 shows the semiquantitative estimation of clay mineral species elucidated from the fine fraction (<2 μm). It appeared that illite (31–64%) and kaolinite (12–19%) are the major clay minerals with minor amounts of smectite (5–12%)

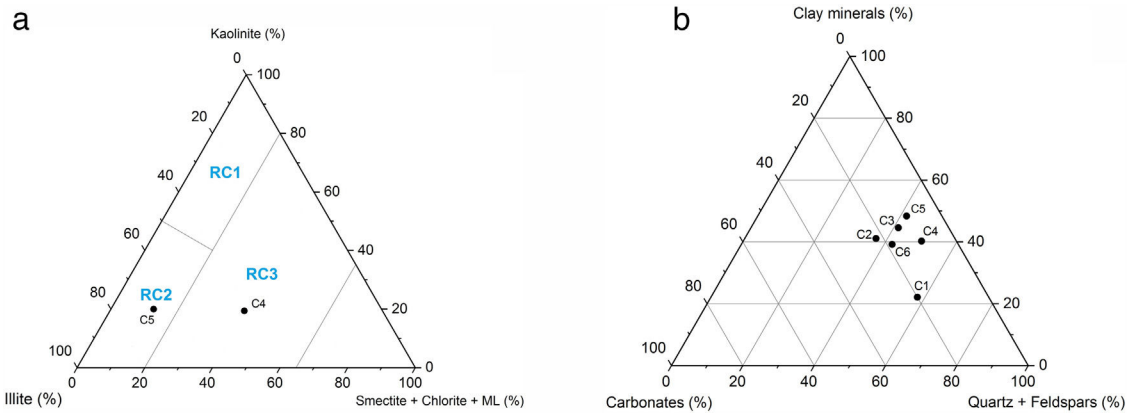

Fig. 3 – (a) Classification of red-firing clays (C4 and C5) according to amount of clay minerals, (b) Classification of the studied clays based on Strazzera ternary diagram.

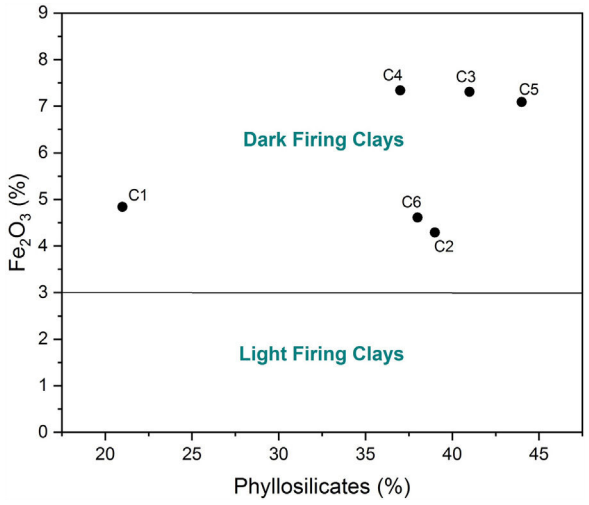

Fig. 4 – Classification of the studied clays according to amount of iron oxides.

Table 3 – IR bands assigned to the minerals found in C5 clay.

Bands	
IR Frequencies of clay C5 (cm^{-1})	Identification
3688	υ O—H (kaolinite)
3619	υ O—H (illite)
3541	υ O—H (chlorite)
3406	υ OH (H_2O) (interlayer water)
3281	Iron hydroxide
2921	υ Organic materials
2513	Calcite/dolomite
1650	δ O—H (adsorbed water)
1437	Calcite/dolomite
1028	υ Si—O (SiO_2)
910	δ Al—Al—OH
775	Quartz
712	Calcite/dolomite
531	δ Si—O—Al (clay minerals)

and chlorite (4–20%). Fig. 3a confirms that the C5 clay sample can be attributed to the RC2 group [13] where illite-mica exceeded 50% of phyllosilicates, and the amount of smectite, interstratified IS and chlorite is within 20%. In contrast, C4 clay sample belongs to RC3 group, a group where the amount of chlorite and mixed layer minerals associated to illite is over 20% of the total of phyllosilicates. According to the Strazzera ternary diagram [36,37] (Fig. 3b), the studied clays (C2–C6) were suitable for structural clay products and clay roofing tiles.

An overall comparison of the various clays revealed clear differences in the chemical and mineralogy composition. For instance, carbonates content very clearly distinguished the marly materials (C1, C2, C3 and C6) from the red clays (C4 and C5). More specifically, calcite and dolomite predominate in the marly-clays (with an average ratio of 10:1 in C3). Feldspar was represented by plagioclase and K-feldspar (C6) and chlorite was absent in C5 clay.

Chemical composition and loss on ignition for raw clays and its fine fraction (i.e., <2 μm sized fraction) are shown in Table 2. The main elements as oxides are silica (SiO_2), alumina (Al_2O_3), iron (Fe_2O_3), and calcium (CaO), whereas potassium (K_2O), magnesium (MgO), sodium (Na_2O), manganese (MnO), and titanium (TiO_2) are present in moderate quantities. The higher Fe_2O_3 content (> 3%) could give all samples a reddish colour after firing, and made them appropriate for dark products (Fig. 4) [13]. In ceramics, colour depends on the ratio between the amounts of iron and calcium that was 5.09 for C4 and 2.63 for C5 [38]. Relatively high mass ratio of Al_2O_3/SiO_2 for C5 clay (0.48) indicated high amount of clay minerals and low content of quartz (Fig. 5a and b). Calcium was significant for C3 and C6 (~9.07%), reflecting the presence of calcite, as described earlier. In addition, the presence of large amounts of fluxes as well as CaO, Na_2O and TiO_2 increased the amount of liquid phase at a lower firing temperature. Loss on ignition ranged between 8.23 and 15.01% because of the elimination of both adsorbed and crystalline water, the combustion of organic matter and the decomposition of carbonates. With the exception of C5 clay, the LOI correlated well with the percentage of carbonates/clay minerals (Fig. 6).

FTIR spectrum of C5 clay showed the existence of organic matter with its broad band at 2921 cm^{-1} (Table 3). Infrared absorption properties of kaolinite and illite corresponding

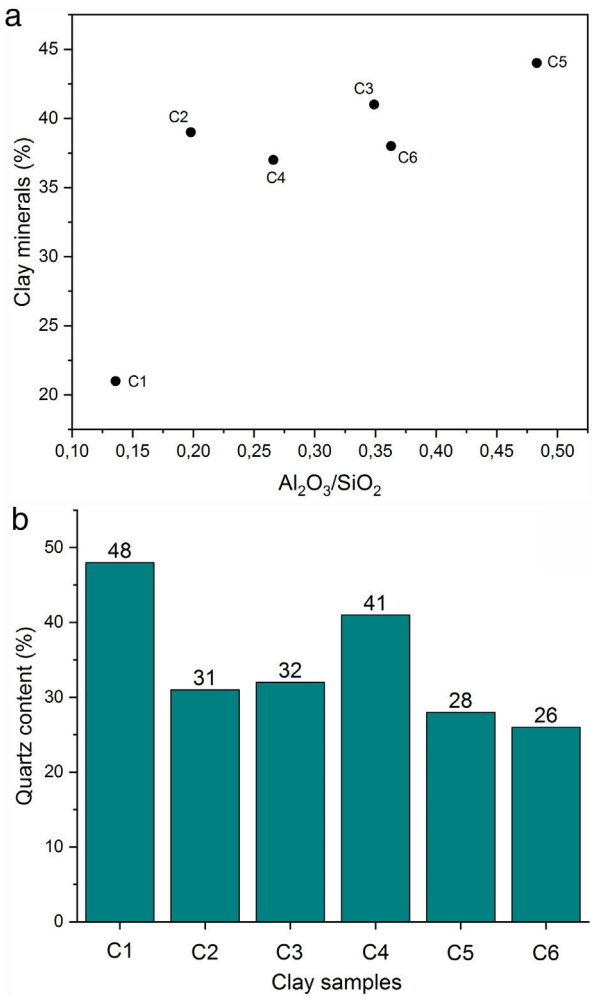

Fig. 5 – (a) Correlation between alumina-silica ratio and clay mineral content; (b) Quartz content in the studied clays.

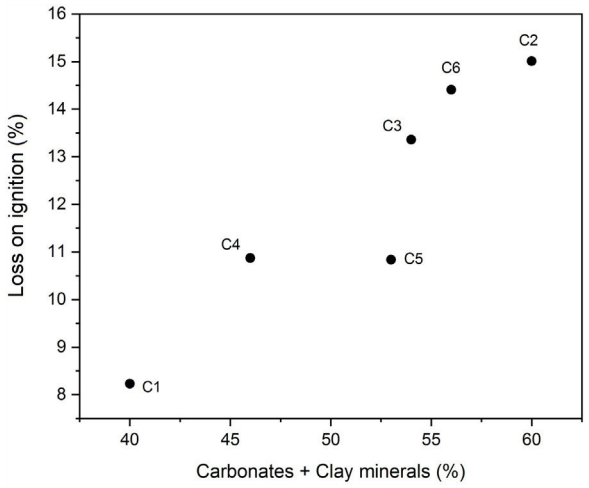

Fig. 6 – Correlation between 'carbonates + clay minerals' and loss on ignition.

to O-H bands were observed at 3688 and 3619 cm^{-1} respectively. Quartz was detected at 775 cm^{-1}. The same table shows the presence of chlorite characterized by the band O-H at 3541 cm^{-1}; water band appeared at 1650 cm^{-1} and iron hydroxide at 3281 cm^{-1} [22,39]. Fig. 7 shows the SEM images of a representative clay, indicating the fine crystalline particles with less than 5 μm-sized particles.

Particle size distribution was variable with clay fractions from 28 to 72%, silt from 25 to 56%, and sand from 3 to 16% (Table 4). Amongst all samples, C5 exhibited the highest clay contents (72 wt.% of the less than 4 μm), but not C1 that showed higher coarse particles (16 wt.%). All the TOC values of the samples were high (1.8–2.5%), except for C4 and C5, which was about 0.55 wt.%. Based on the sand-silt-clay ternary diagram, almost all of the samples (C2–C6) are classified as silty clay, except C1 sample (Fig. 8) [36,37].

Plasticity parameters, plotted on a Holtz and Kovacs diagram [40,41] indicated that these clays have variable plasticity. This is easily understandable from the particle size distribution and mineral compositions (Tables 1 and 4). In fact, low quartz and organic content in the original clay (28% and 0.5% respectively), the presence of smectite (12%) and high illite content (64%) enhanced plasticity, as was the case of C5 clay (plasticity index 32). Both C5 and C6 samples fell within the illitic clay area of the diagram, thus, considered as higher plasticity materials. The low plasticity indices for both C1 and C4 samples proved the high quartz content. Plastic properties of the studied clays are shown in the relevant diagrams (Holtz and Kovacs, and Casagrande diagram) of Fig. 9. Overall, C2, C5 and C6 clay samples showed acceptable extrusion properties. Plasticity of a given clay is an important parameter generally used to determine the adequate application of the clay body. Various factors affected the plastic properties such as origin of geological formation, mineral composition, particle size distribution, impurities (nonclay minerals), and organic matter [42]; they should be take care of during the preparation of ceramic bodies, as the case in the current work.

According to ceramic clay classification of Dondi et al. [13], dark-firing clay are related to iron oxide and carbonates content, in addition to the coarse fraction (>63 μm). C1 was a clayey silt due to its high coarse-grained fraction (16%). C2, C3 and C6 were marls due to high carbonate content (from 13 to 21%). C4 and C5 samples are red clays due to low carbonate content (9%) and coarse-grained fraction. Fig. 10 shows the suitability of different clays from El Jadida city to ceramic products. It can be found that both C5 and C6 are suitable for hollow products, C2 and C4 for roofing tiles and masonry bricks and C1 for common bricks of the Winkler presentation [36]. C3 sample did not conform any product specifications and would require beneficiation.

Table 5 shows the weight losses in the temperature range set during thermogravimetric analysis. The loss below 400 °C can be attributed to the release of physically adsorbed water and the combustion of organic materials present in the raw clays. Between 400 and 800 °C, a second weight loss (6.33 to 13.21%) was explained by the dehydroxylation of clay minerals and decomposition of carbonates. Beyond 800 °C, only C1, C4 and C5 showed a slight weight loss. The total weight loss of C1, C2, C3, C4, C5 and C6 were 10.18; 17.27; 14.04; 12.56; 12.12 and 16.00%, respectively, suggesting 1100 °C as a compromising temperature for stable sintering materials.

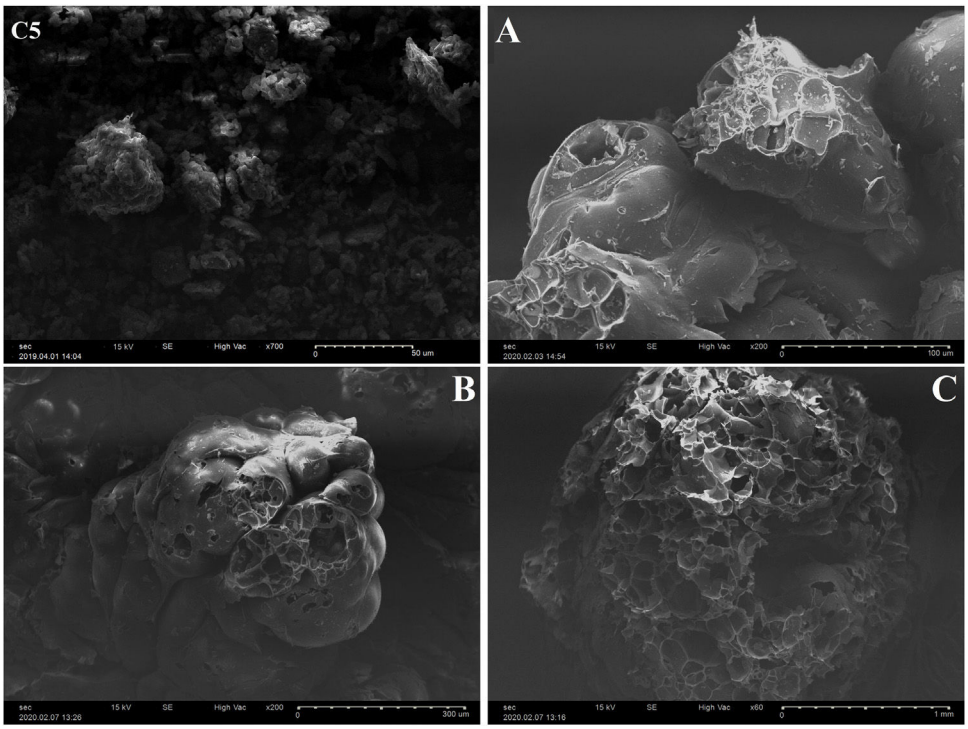

Fig. 7 – SEM micrographs of C5 clay and EP at ambient temperature. A: <200 μm, B: 400–800 μm and C: 1000–2500 μm.

Table 4 – Carbonate content, grain-size and specific surface area results of the studied clay.

	C1	C2	C3	C4	C5	C6
Total $CaCO_3$ (wt.%)	14.03	14.66	12.75	8.21	9.14	17.01
Particle size distribution (wt.%)						
Clay (<4 μm)	28	60	65	50	72	58
Silt (4–63 μm)	56	29	30	38	25	28
Sand (>63 μm)	16	11	5	12	3	14
Specific surface area (m^2/g)	18.3	43.9	44.4	38.9	51.2	36.6
Total organic content (wt.%)	2.1	2.5	1.3	0.6	0.5	1.8

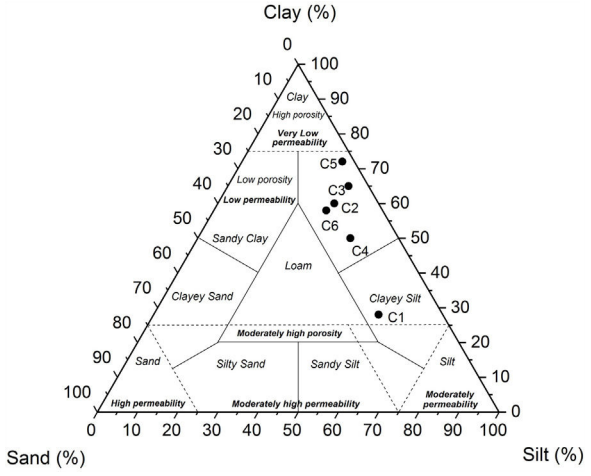

Fig. 8 – Sand-silt-clay ternary diagram of the studied clay samples.

The distribution of potassium was attributed to illite/mica, as confirmed by the positive correlation between illite and potassium contents (Fig. 11). This was expected from the structural formula of Illite. In ceramic industry, clays with high quartz content are not preferred because of its potential not desired reactions with other oxides. It may produce undesirable phases at low firing temperatures. Our preliminary results have shown that C5 clay was the most favourable sample that can be used for ceramic preparation, besides C3, C4 and C6 clays that can be used in wall tiles if they are mixed with other plastic clays [43]. Thus, subsequent study will focus on testing the effect of EP addition on the technological properties of the final ceramic product.

Perlite is a glassy volcanic rock of rhyolitic composition usually containing a small amount of combined water. Raw perlite when heated to an appropriate temperature (above 870 °C) expands and transforms into a white cellular material of low bulk density (40–110 kg/m^3) (Fig. 7). The particles are hollow and porous with many shapes. The microstructure of EP is characterized by open pores (small channels which form a thick network) and closed pores (isolated holes and

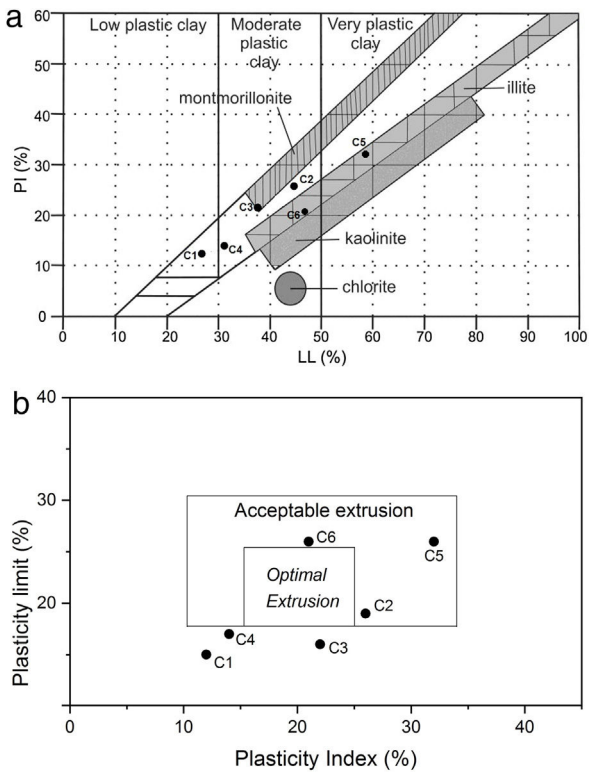

Fig. 9 – Position of dark clay-rich materials: (a) on the Holtz and Kovacs diagram and (b) on workability chart.

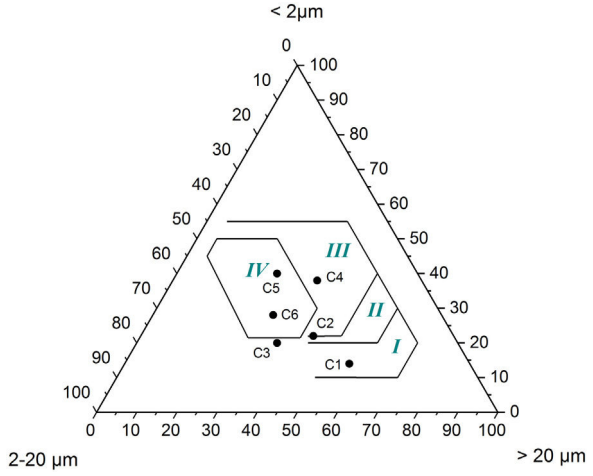

Fig. 10 – Winkler diagram for the studied clay-rich samples. Fields are defined as: (I) common bricks, (II) vertically perforated bricks, (III) roofing tiles and masonry bricks, and (IV) hollow products.

cells). This structure gives excellent insulation properties, low density and high porosity of materials [9,10]. Moreover, EP shows chemical inertness, fire resistance and high absorption of sound. The used EP consists mainly of SiO_2, Al_2O_3 and lesser amounts of several metal oxides such as sodium, potassium, iron, calcium and magnesium (Table 2).

In XRD, an analysis of expanded perlite the glassy behaviour was observed (Fig. 12a). The same pattern also showed the presence of quartz and cristobalite peaks. FTIR spectrum (Fig. 12b) showed the presence of two weak bands located at 782 and 1518 cm^{-1} due to the deformation of Al—O—Si and the elongation vibration of Si—O—Si group, respectively. An intense band located at 1011 cm^{-1} characterizing the elongation vibration of the Si—O group was suggested high silica content. A very fine elongation vibration at 3616 cm^{-1} attributed to the O—H group was also observed [44,45].

Characterization of ceramics

Technological properties of the prepared ceramic samples are reported in Table 6. Linear firing shrinkage, water absorption, and flexural strength have been frequently used as quality and process control parameters in the production of structural ceramics (e.g., floor and wall tiles). A moderate water absorption (9.5%) and higher linear shrinkage (3.04%) were observed. According to the European Standard NF EN159 (1991), ceramic without EP can be classified into group BIIb (B for pressing). The vitrification is marked by acceptable bending strength (20.8 MPa). Good mechanical properties of ceramic product without EP is required for a better casting of the sample; the shape of the pores and the crystalline/vitreous phase ratio are also determining factors. The presence of a crystalline phase (anorthite) in the ceramic matrix provides a good fired mechanical strength to the specimene. Dondi et al. [46] reported a classification diagram using water absorption and bending strength (Fig. 13). C5 clay seemed to satisfy the requirements for the production of cottoforte ceramics. These results show similar characteristics to other clays, which are currently used in Morocco [6,16,17,22,25,47–50].

Depending on the increase in the perlite addition and porosity content, the bending strength values of the samples progressively decreased from 20.8 to 7.4 MPa. The thermal conductivities and bulk densities were reduced by 63% and 33% respectively, with increasing perlite addition. It should be noted that water absorption, linear shrinkage, and thermal conductivity values are always interdependent, and, therefore, the lower the water absorption, the lower the linear shrinkage, and the greater the thermal conductivity. $C10_A$ was suitable

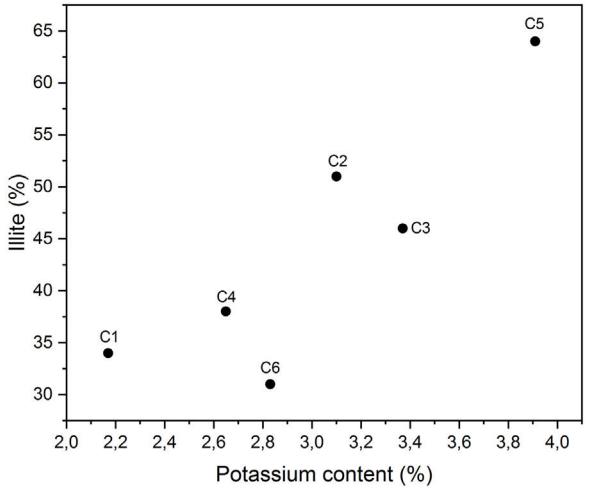

Fig. 11 – Correlation between potassium and illite of the studied clays.

Table 5 – The mass losses (%) registered on TG curves.

Samples	95–200 °C	200–400 °C	500–800 °C	800–1100 °C
C1	0.83	1.91	6.33	1.11
C2	1.69	2.88	12.70	–
C3	0.52	3.11	10.41	–
C4	0.91	1.56	8.94	1.15
C5	0.58	0.91	9.62	1.01
C6	1.12	1.67	13.21	–

for both monoporosa and cottoforte. Properties of $C10_B$ and $C20_A$ corresponded well with those of majolica and cottoforte respectively. It was observed that the colour of the fired samples does not change with increasing the amount of EP addition up to 10%. For $C10_A$ sample, the mechanical properties and thermal conductivity were similar compared to C0 sample. This is possibly due to the vitrified structure created by fine perlite (<200 μm), which reduced the effect of EP. During liquid phase formation, the liquid surface tension and capillarity helped particles to agglomerate and reduce porosity [9].

Ultrasonic pulse velocity of materials is commonly used in the mechanical characterization of materials and prediction of strength values. The propagation velocity of the waves Vp (Fig. 14) decreases with increasing particle size fraction of EP. This could be explained directly by increasing of the pores.

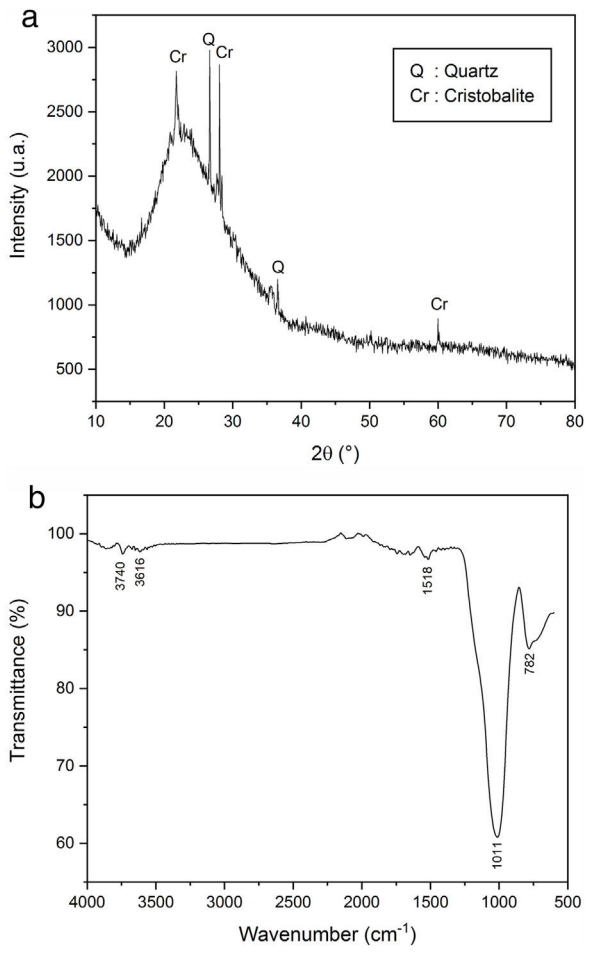

Fig. 12 – XRD patterns (a) and infrared spectrum (b) of EP.

It can be noted that the particle size affects the propagation velocity more than the amount of expanded perlite. This is illustrated for $C20_A$ which has velocity values greater than $C10_C$. For C0 and $C10_A$, almost similar velocities are measured. Fig. 15 shows the change in the porosity versus EP content. Ceramic specimen without EP had a homogeneous and dense structure, but addition of EP (20%) clearly enhanced

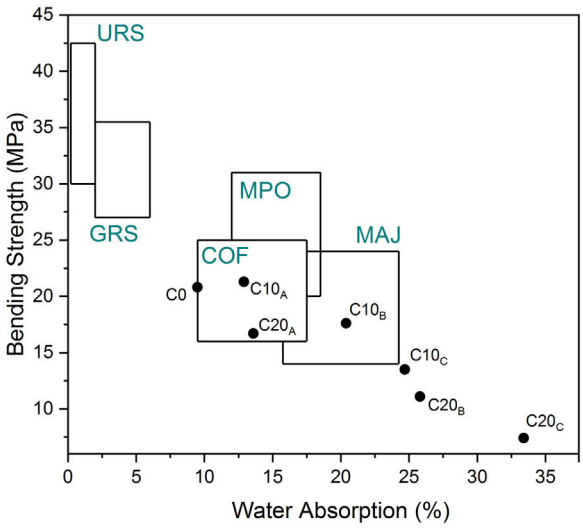

Fig. 13 – Water absorption versus bending strength for elaborated ceramics. MAJ: majolica, COF: cottoforte, MPO: monoporosa, GRS: glazed red stoneware, URS: unglazed red stoneware.

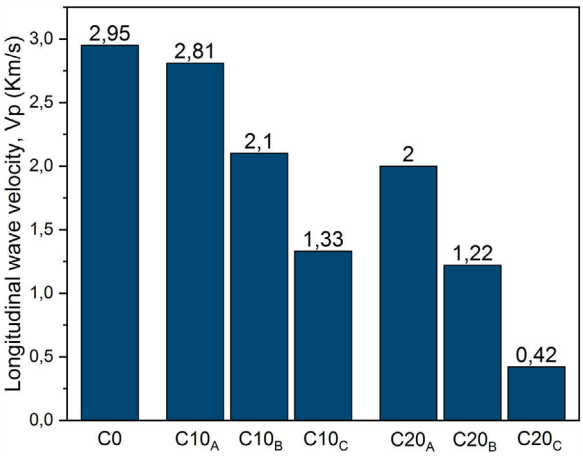

Fig. 14 – Vp values of the fired samples.

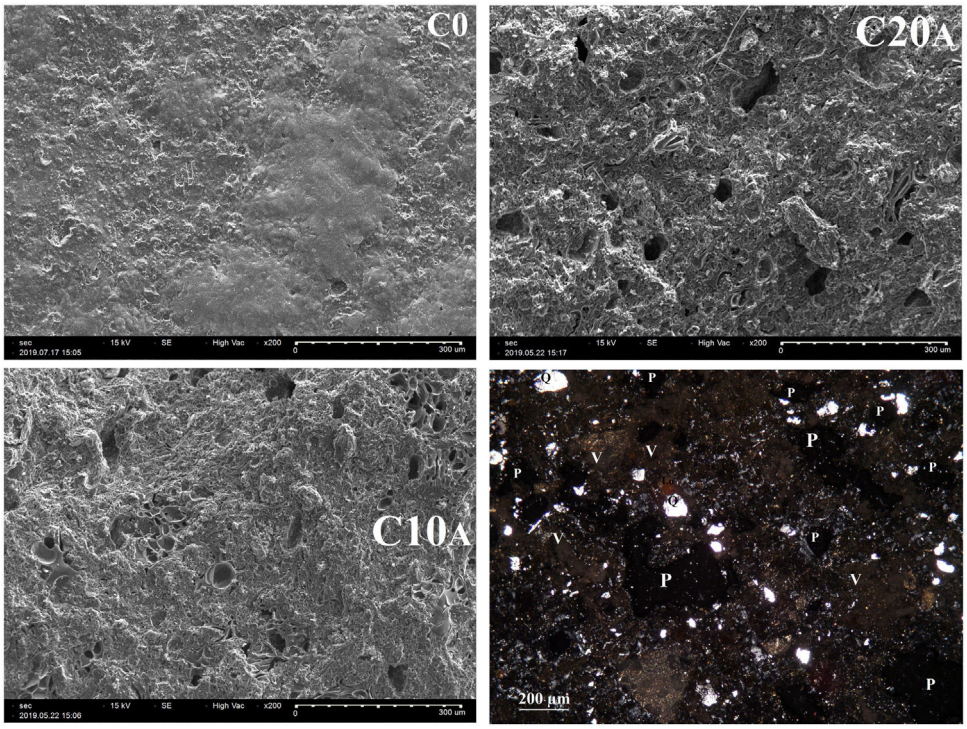

Fig. 15 – SEM micrographs of ceramics fired at 1100 °C with different EP content, and microstructural analysis of the $C20_A$ sample taken with polarized microscopy light (APL). P: Porosity, I.o: Iron oxide, Q: Quartz, V: Vitreous phase.

its porosity whose size is between 20 and 60 μm. Calcite and dolomite minerals also contributed to a lesser extent, to the formation of porous structure. Upon thermal treatment, the loss of CO_2 may generate some bubbles to produce CaO-rich particles with a porous structure [22,32]. The pores are often isolated and have globular shape. The same figure illustrates the microscopic observations of sample $C20_A$ using polarized light (APL). The studied material appears heterogeneous with some anisotropic crystals, opaque phases, amorphous areas and porosity. The anisotropic minerals correspond to quartz crystals, which are xenomorphic, show a rolling extinction, and are often cracked. The opaque phases are frequently iron oxides.

A variety of mineral modifications occurred in C5 ceramic; kaolinite, illite-smectite, plagioclase and K-feldspars disappeared at 550, 950 and 1000 °C, respectively (Fig. 16). Quartz and hematite were the main original minerals to resist to the high temperature. Assemblage of the newly formed minerals from C5 clay included potassium aluminium silicate (sanidine), gehlenite ($Ca_2Al(AlSiO_2)$), anorthite ($CaAl_2Si_2O_8$), cristobalite and spinel crystalline phases. These minerals began to crystallize after the destruction of phyllosilicates structure (kaolinite, illite and smectite), k-feldspar, calcite and dolomite. Decarbonation produced CaO that will react with decomposed silicate sheets to generate neoformed calcium minerals (Ca-silicates), including gehlenite and anorthite. Fired sample contained Mg-rich spinel, probably derived from the dehydroxylation of smectite, phyllosilicate minerals rich in MgO. Spinel was formed by the reaction: $MgO + Al_2O_3 \rightarrow MgAl_2O_4$.

Addition of EP caused the loss of all the minerals present in C0 sample (Table 7). Quartz was the most abundant phase in C0, $C10_A$ and $C20_A$. Vitreous content is about 14% for the sample C0; it increased to 37% for the sample $C20_A$. This is directly caused by the glassy behaviour imported by perlite and the dissolution in the amorphous phase. It is noted from Fig. 17 that different samples sintered at 1100 °C having dielectric constant values lie from ~1.738 for C0 to ~3.117 for C20 when measured within the frequency range of 2–20 GHz at room temperature. The dielectric constant value increases with increasing EP content in the base composition.

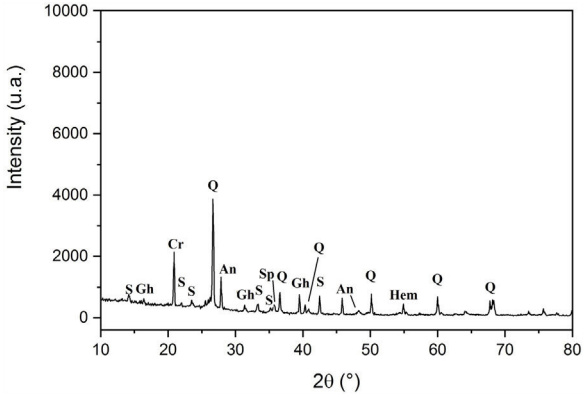

Fig. 16 – XRD patterns of sample C0 fired at 1100 °C (Q: Quartz, Cr: Cristobalite, S: Sanidine, Gh: Gehlenite, An: Anorthite, Hem: Hematite, Sp: Spinel).

Table 6 – Measured values of the ceramics fired at 1100 °C.

	0% of EP	10% of EP			20% of EP		
	C0	<200 μm $C10_A$	400–800 μm $C10_B$	1000–2500 μm $C10_C$	<200 μm $C20_A$	400–800 μm $C20_B$	1000–2500 μm $C20_C$
Porosity (%)	20.2 20.2	18.9	25.7 26.4	32.6	22.3	34.1 34.3	46.5
Density (g/cm^3)	1.92 1.92	1.92	1.81 1.79	1.66	1.7	1.56 1.51	1.28
Water absorption (%)	9.5 9.5	12.9	20.4 19.3	24.7	13.6	25.8 24.3	33.4
Shrinkage (%)	3.04 3.04	3.66	3.66 3.67	3.69	4.28	4.82 5.01	5.95
Bending strength (MPa)	20.8 ± 20.8 ±	21.3	17.6 17.46	13.5	16.7	11.1 11.7	7.4
Tensile strength (MPa)	11.9 11.9	12.3	10.6 10.1	7.4	10.2	6.7 7.2	4.7
Thermal conductivity (W/m K)	0.79 ± 0.01 0.79	0.80 ± 0.01	0.61 ± 0.01 0.64	0.53 ± 0.01	0.61 ± 0.01	0.35 ± 0.01 0.41	0.29 ± 0.01
Abrasion resistance (cm^2/g)	4.4 4.4	4.9	4.3 4.13	3.2	3.7	3.5 3.23	2.5
Colour	2.5YR/4/8 Red		2.5YR/4/8 Red			2.5YR/5/6 Light red	

Table 7 – Phases composition of the ceramic bodies fired at 1100 °C.

	C0	$C10_A$	$C20_A$
Quartz	27	25	21
Cristobalite	5	6	8
Sanidine	20	19	16
Gehlenite	14	10	6
Anorthite	8	6	5
Hematite	7	5	4
Spinel	5	4	3
Vitreous phase	14	25	37

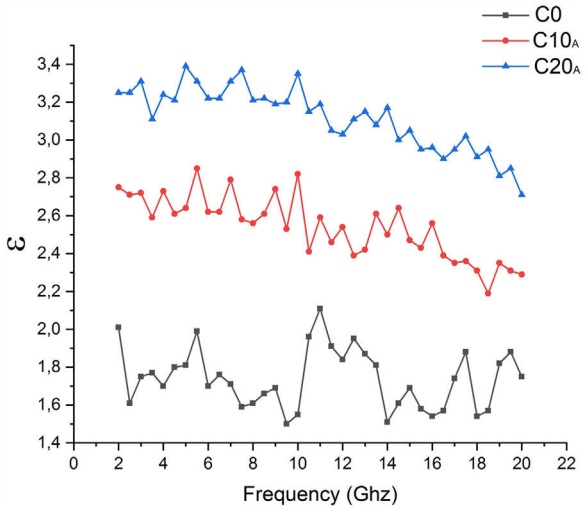

Fig. 17 – Dielectric constant of fired sample.

Conclusions

This study has been performed to evaluate the potential of using raw clayey materials from El Jadida area (Coastal Meseta, Morocco) to supply ceramic industry. The characteristics of the six representative clay samples (C1–C6) and their effects on ceramic properties led to the conclusions presented in the table below. Chemical analysis revealed high amounts of oxides, mainly SiO_2, Al_2O_3, Fe_2O_3, CaO and MgO. Those results were confirmed by mineralogical study of the raw materials in favour of high illite, quartz and carbonate contents. The oxides analysis showed that the higher the Al_2O_3/SiO_2 ratio, the higher the content of clay minerals. Addition of expanded perlite for the production of porous ceramics, strongly affected the microstructure, porosity and other technological properties of the fired products. Thus, the use of EP as aggregates allowed a gradual increase in the porosity of the prepared ceramic specimen. To conclude, the use of C5 clay sample with 20% of coarse EP provided the optimized conditions for a highly porous material ($P = 46.5\%$, $d = 1.28$ g/cm^3), but not higher than 2.5 mm-sized EP sample. Finally, it can be stated that ferruginous clays from El Jadida area were found suitable for extraction to supply ceramic industry for a sustainable large scale quarrying activity.

This study confirms the fundamental role that research and development (R & D) can play in ceramics companies in improving quality of their finished products. The general interest in this study is in particular, the possibility of correcting ordinary clays by adding expanded perlite to produce innovative lightweight and insulating ceramics. This will certainly contribute to: (1) the development of the local raw material and therefore the sustainable socio-economic development of the local population and (2) the innovation in construction

Table 8 – Summary table.

Samples	Fe_2O_3 content (%)	Type	Carbonate content (%)	Type of sample	Type of clay	Al_2O_3/SiO_2	Clay minerals content (%)	Flexural strength at 1100 °C (MPa)	Strazzera ternary diagram	Quartz content (%)	Plasticity	Strazzera ternary diagram	Industrial applica-tions
C1	4.84		19	Marl	–	0.13	21	15.3	–	48	Low plastic clay	Clayey silt	Common bricks
C2	4.29	Dark firing clays	21	Marl	–	0.19	39	14.2	Structural clay products & clay roofing tiles	31	Moderate plastic clay	Silty clay	Roofing tiles and masonry bricks
C3	7.31		13	Marl	–	0.35	41	16.1		32	Moderate plastic clay		Wall tiles
C4	7.34		9	Red clay	RC3	0.26	37	18.5		41	Moderate plastic clay		Roofing tiles and masonry bricks
C5	7.09		9	Red clay	RC2	0.48	44	20.8		28	Very plastic clay		Hollow products
C6	4.61		18	Marl	–	0.36	38	15.6		26	Moderate plastic clay		Hollow and wall tiles

materials allowing the development of the quality of buildings especially in terms of energy comfort (Table 8).

REFERENCES

[1] A. Elgamouz, N. Tijani, I. Shehadi, K. Hasan, M.A. Kawam, Characterization of the firing behaviour of an illite-kaolinite clay mineral and its potential use as membrane support, Heliyon 5 (2019) e02281.
[2] A. Elgamouz, N. Tijani, I. Shehadi, K. Hasan, M.A. Kawam, Dataset of multiple methodology characterization of an illite-kaolinite clay mineral for the purpose of using it as ceramic membrane supports, Data Brief 29 (2020) 105300.
[3] Applied ceramic technology. Volume I. Editrice La Mandragora s.r.l. 2005.
[4] I. El Amrani El Hassani, C. Sadik, Geology and mineralogy of clays for nanocomposites: state of knowledge and methodology, in: Nanoclay Reinforced Polymer Composites, 2016, pp. 85–113.
[5] H. Driouiche, Résultats d'essais technologiques pour briqueterie effectués sur deux échantillons provenant de la région de Safi. Rapport SRG/MAR/N° 39 bis, Service régional de la géologie, Marrakech (1984) 4.
[6] C. Sadik, I. El Amrani, A. Albizane, Composition and ceramic characteristics of cretaceous clays from Morocco, Adv. Sci. Technol. 92 (2014) 209–214.
[7] F. Guerraoui, M. Zamama, M. Ibnoussina, Caractérisation minéralogique et géotechnique des argiles utilisées dans la céramique de Safi (Maroc), African, J. Sci. Tech. Sci. Eng. 9 (2008) 1–11.
[8] A.M. Rashad, A synopsis about perlite as building material – a best practice guide for civil engineer, Constr. Build. Mater. 121 (2016) 338–353.
[9] L.F. Dutra, M.E. Freitas, A.C. Grillet, N. Mendes, M. Woloszyn, Microstructural characterization of porous clay-based ceramic composites, Materials 12 (2019) 946.
[10] C. Sadik, A. Albizane, I. El Amrani, Production of porous firebrick from mixtures of clay and recycled refractory waste with expanded perlite addition, J. Mater. Environ. Sci. 4 (6) (2013) 981–986.
[11] H. Yildizay, H. Kadioğlu, Effects of perlite addition on the structure of hard porcelain glaze, J. Aust. Ceram. Soc. 54 (2018) 369–375.
[12] D.A. Brosnan, Alumina–silica brick, in: C.A. Schacht (Ed.), Refractories Handbook, Marcel Dekker Inc., New York, 2004, pp. 79–107.
[13] M. Dondi, M. Raimondo, C. Zanelli, Clays and bodies for ceramic tiles: reappraisal and technological classification, Appl. Clay. Sci. 96 (2014) 91–109.
[14] Commission européenne. Fabrication des céramiques. 2007.
[15] Applied ceramic technology. Volume II. Editrice La Mandragora s.r.l. 2005.
[16] C. Sadik, I. El Amrani, A. Albizane, Influence de la nature chimique et minéralogique des argiles et du processus de fabrication sur la qualité des carreaux céramiques, MATEC. Web. Conf. 2 (2012) Article ID: 01016.
[17] N. El Yakoubi, M. Aberkan, M. Ouadia, Potentialité d'utilisation d'argiles marocaines de Jbel Kharrou dans l'industrie céramique, C.R. Geosci. 338 (2006) 693–702.
[18] H. Elomari, B. Achiou, M. Ouammou, A. Albizane, J. Bennazha, S. Alami Younssi, I. El Amrani, Elaboration and characterization of flat membrane supports from Moroccan clays. Application for the treatment of wastewater, Desal. Water. Treat. 1 (2015) 20298–20306.
[19] M. El Ouahabi, L. Daoudi, F.D. Vleeschouwer, R. Bindler, N. Fagel, Potentiality of clay raw materials from northern morocco in ceramic industry: Tetouan and Meknes areas, J. Miner. Mater. Charact. Eng. 2 (2014) 145–159.
[20] M. El Ouahabi, L. Daoudi, N. Fagel, Preliminary mineralogical and geotechnical characterization of clays from morocco: application to ceramic industry, Clay. Miner. 49 (2014) 1–17.
[21] C. Sadik, I. El Amrani, A. Albizane, Composition and refractory properties of mixtures of Moroccan silica-alumina geomaterials and alumina, New J. Glass. Ceram. 3 (2013) 59–66.
[22] A. Manni, A. El Haddar, I. El Amrani El Hassani, A. El Bouari, C. Sadik, Valorization of coffee waste with Moroccan clay to produce a porous red ceramics (class BIII), boletín de la sociedad española de cerámica y vidrio 58 (2019) 211–220.
[23] A. El Haddar, A. Manni, A. Azdimousa, I. El Amrani El Hassani, A. Bellil, C. Sadik, N. Fagel, M. El Ouahabi, Elaboration of a high mechanical performance refractory from halloysite and recycled alumina, J. Span. Ceram. Glass Soc. (2019).
[24] C. Sadik, A. Manni, S. El Kalakhi, I. El Amrani, Preparation and characterization of possible basic ceramics from Moroccan magnesite, J. Aust. Ceram. Soc. 55 (2019) 415–423.
[25] A. Manni, A. Elhaddar, A. El Bouari, I. El Amrani, C. Sadik, Complete characterization of Berrechid clays (Morocco) and manufacturing of new ceramic using minimal amounts of feldspars: Economic implication, Case Stud. Construct. Mater. 7 (2017) 144–153.
[26] C. Sadik, I. El Amrani, O. Moudden, A. El Bouari, Review on the elaboration and characterization of ceramics refractories based on magnesite and dolomite, J. Asian Ceram. Soc. 4 (2016) 219–233.
[27] C. Sadik, I. El Amrani, A. Albizane, Processing and characterization of alumina-mullite ceramics, J. Asian Ceram. Soc. 2 (2014) 310–316.
[28] M. Hajjaji, S. Kacim, M. Boulmane, Mineralogy and firing characteristics of a clay from the valley of Ourika (Morocco), Appl. Clay Sci. 21 (2002) 203–212.
[29] D. Frizon de Lamotte, A. Crespo-Blanc, B. Saint-Bezar, M. Comas, M. Fernadez, H. Zeyen, H. Ayarza, C. Robert-Charrue, A. Chalouan, M. Zizi, A. Teixell, M.L. Arboleya, F. Alvarez-Lobato, M. Julivert, A. Michard, TRASNSMED-transect I [Betics, Alboran Sea, Rif, Moroccan Méseta, High Atlas, Jbel Saghro, Tindouf basin], in: W. Cavazza, F. Roure, W. Spakman, G.M. Stampfli, P.A. Ziegler (Eds.), The TRANSMED Atlas – The Mediterranean Region from Crust to Mantle, Springer, Berlin, 2004.
[30] G.W. Brindley, Quantitative X-ray mineral analysis of clays, in: G.W. Brindley, G. Brown (Eds.), Crystal Structures of Clay Minerals and Their X-ray Identification, Monograph 5. Mineralogical Society, London, 1980, pp. 411–438.
[31] A. Casagrande, Classification and identification of soils, ASCE Transactions Paper No. 2351 (1947) 901–991.
[32] M. Sutcu, S. Akkurt, The use of recycled paper processing residues in making porous brick with reduced thermal conductivity, Ceram. Int. 35 (2009) 2625–2631.
[33] ASTM C373-88, Standard test method for water absorption, bulk density, apparent porosity, and apparent specific gravity of fired whiteware products. 15-02, Glass Ceram (2006).
[34] ASTMC 326-03, Standard test method for drying and firing shrinkages of ceramic whiteware clays. ASTM International, West Conshohocken (2003).
[35] A. Oushabi, S. Sair, Y. Abboud, O. Tanane, A. El Bouari, An experimental investigation on morphological, mechanical and thermal properties of date palm particles reinforced polyurethane composites as new ecological insulating materials in building, Case Stud. Constr. Mater. 7 (2017) 128–137.
[36] B. Semiz, Characteristics of clay-rich raw materials for ceramic applications in Denizli region (Western Anatolia), Appl. Clay Sci. 137 (2017) 83–93.
[37] B. Strazzera, M. Dondi, M. Marsigli, Composition and ceramic properties of tertiary clays from southern Sardinia (Italy), Appl. Clay Sci. 12 (1997) 247–266.

[38] C. Fiori, B. Fabbri, G. Donati, I. Venturi, Mineralogical composition of clay bodies used in the Italian tile industry, Appl. Clay Sci. 4 (1989) 461–476.
[39] M. Hajjaji, Mineralogy and thermal transformation of clayey materials from the district of Marrakech, Morocco, Comunicações Geológicas 101 (1) (2014) 75–80.
[40] S. Mahmoudi, A. Bennour, E. Srasra, F. Zargouni, Characterization, firing behavior and ceramic application of clays from the Gabes region in south Tunisia, Appl. Clay Sci. 135 (2017) 215–225.
[41] R.D. Holtz, W.D. Kovacs, An Introduction to Geotechnical Engineering, Prentice- Hall, Inc., New Jersey, 1981.
[42] H.H. Murray, Applied Clay Mineralogy. Developments in Clay Science 2, Elsevier B.V., 2007.
[43] A. Escardino Benlloch, Single-fired ceramic wall tile manufacture, Int. Ceram. J. (1992) 111–140.
[44] Z. Rezaei, S. Jafarirad, M. Kosari-Nasab, Modulation of secondary metabolite profiles by biologically synthesized MgO/perlite nanocomposites in Melissa officinalis plant organ cultures, J. Hazard. Mater. 380 (2019) 120878.
[45] J. Rodriguez, F. Soria, H. Geronazzo, H. Destefanis, Modification and characterization of natural aluminosilicates, expanded perlite, and its application to immobilise α-amylase from A. oryzae, J. Mol. Catal. B: Enzym. 133 (2016) S259–S270.
[46] M. Dondi, G. Guarini, P. Ligas, M. Palomba, M. Raimondo, I. Uras, Chemical, mineralogical and ceramic properties of kaolinitic materials from the Tresnuraghes mining district (Western Sardinia, Italy), Appl. Clay Sci. 18 (2001) 145–155.
[47] L. Mesrar, A. Benamar, R. Jabrane, Study of Taza's Miocene marl applications in heavy clay industry, Bull. Eng. Geol. Environ. (2020) (in press).
[48] M. El Ouahabi, H. El Boudour El Idrissi, L. Daoudi, M. El Halim, N. Fagel, Moroccan clay deposits: physico-chemical properties in view of provenance studies on ancient ceramics, Appl. Clay Sci. 172 (2019) 65–74.
[49] M. Monsif, A. Zerouale, N.I. Kandri, M. Mozzon, P. Sgarbossa, F. Zorzi, F. Tateo, S. Tamburini, E. Franceschinis, S. Carturan, R. Bertani, Chemical–physical and mineralogical characterization of ceramic raw materials from Moroccan northern regions: Intriguing resources for industrial applications, Appl. Clay Sci. 182 (2019) 105274.
[50] M. Mouiya, A. Bouazizi, A. Abourriche, Y. El Khessaimi, A. Benhammou, Y. El hafiane, Y. Taha, M. Oumam, Y. Abouliatim, A. Smith, H. Hannach, Effect of sintering temperature on the microstructure and mechanical behavior of porous ceramics made from clay and banana peel powder, Results Mater. 4 (2019) 100028.